SCIENTIFIC REPORTS

OPEN

SUBJECT AREAS:
CELL BIOLOGY
IMMUNOLOGY

Received
10 September 2014

Accepted
11 December 2014

Published
14 January 2015

Correspondence and requests for materials should be addressed to J.D.H. (john.hayball@unisa.edu.au)

Scrutinizing calcium flux oscillations in T lymphocytes to deduce the strength of stimulus

Susan N. Christo[1,2], Kerrilyn R. Diener[1,2,3], Robert E. Nordon[4], Michael P. Brown[1,2,5,9], Hans J. Griesser[6], Krasimir Vasilev[7], Farid C. Christo[8] & John D. Hayball[1,2,9]

[1]Experimental Therapeutics Laboratory, Hanson Institute, Adelaide, SA 5000, Australia, [2]Sansom Institute and School of Pharmacy and Medical Sciences, University of South Australia, Adelaide, SA 5000, Australia, [3]Robinson Research Institute and School of Paediatrics and Reproductive Health, University of Adelaide, Adelaide, SA 5005, Australia, [4]Graduate School of Biomedical Engineering, University of New South Wales, Kensington, NSW, 2052, Australia, [5]Cancer Clinical Trials Unit, Royal Adelaide Hospital, Adelaide, SA 5000, Australia, [6]Ian Wark Research Institute, University of South Australia, Adelaide, SA 5095, Australia, [7]Mawson Institute, University of South Australia, Adelaide, SA 5000, Australia, [8]Barbara Hardy Institute, University of South Australia, Adelaide, SA 5000, Australia, [9]School of Medicine, University of Adelaide, Adelaide, SA 5005, Australia.

The capture and activation of individual T cells on functionalised surfaces enables real-time analyses of the magnitude and rhythm of intracellular calcium release. Application of Haarlet transformations generate a calcium flux 'threshold', with the frequency of the 'threshold crossings' correlating with the strength of the original T cell stimulus. These findings represent a new method to evaluate graduations in T cell activation in real time, and at a single-cell level.

Interrogating the magnitude and quality of T cell responses[1,2] depends on *ex vivo* analyses of individual T cell function, usually by using T cell antigen receptor-specific tetramers[3,4], with subsequent analysis of their functional potential[5]. Patterns of individual T cell cytokine secretions upon *ex vivo* antigen-specific stimulation is often utilised[3], but despite recent efforts to improve the specificity and consistency of these methods, consensus on the best approach to 'standardise' these types of analyses is lacking[5]. Other functional responses such as cytolytic enzyme release, phenotypic surface marker expression patterns and changes in intracellular calcium (Ca^{2+}) concentration are also commonly used to predict effector characteristics[6], however these approaches only allow for population-based analyses[7], and it is of crucial importance when using *ex vivo* analyses to infer *in vivo* efficacy that functionally-relevant T cells can be distinguished from those that are irrelevant.

Calcium flux is a pivotal signalling event that controls a plethora of T cell functions. Upon T cell receptor (TCR) engagement, formation of the proximal signalling complex facilitates PLCγ1-mediated hydrolysis of PIP_2 into inositol triphosphate (IP_3) and diacylglycerol. When IP_3 binds the IP_3 receptor on the endoplasmic recticulum (ER) membrane, calcium stores are released and trigger store operated calcium entry (SOCE) via calcium-release activated calcium (CRAC) channels[8,9]. This is achieved when the STIM1 molecule in the ER membrane 'senses' stores depletion, and undergoes conformational changes for oligomerisation, and translocation to the plasma membrane (PM). Interactions between STIM1 and the CRAC channel subunits, Orai1 proteins, result in an open channel conformation and subsequent calcium influx[10,11]. The STIM-Orai1 interactions appear as 'puncta' at the ER-PM junction however recent reports describe 'cap-like' structures of highly dense protein regions at the distal end of TCR engagement[12]. The physiological significance of these caps have not been fully elucidated but have been proposed to allow rapid shift in machinery upon additional simulation, or alternatively, may sequester CRAC channels to control calcium flux and downstream T cell responses[12]. This corroborates the highly controlled mechanisms calcium movement in an oscillatory manner, which result from a complex interplay of many receptors and ion channels that can produce specific patterns for directing responses[13–15].

A new method for real-time analyses of intracellular calcium flux in T cells enabling individual and population-based assessment of ligand-induced oscillations is described. Such oscillations occur in different cell types[16], with emerging data suggesting they may be an important regulator of subsequent downstream T cell effector function[17] and contribute to the inherent functional plasticity of T cells. For instance, calcium oscillations are thought to be responsible for driving distinct patterns of gene transcription by triggering differential nuclear localisation of

NFAT and NFκB[18,19]. These oscillations may also sensitise T cells in situations of limited or low affinity antigen[18], with cytolytic activity only instilled in $CD8^+$ T cells after several calcium flux events[2]. Elegant *in vivo* studies of antigen-specific $CD4^+$ T cells also reported that calcium patterns were different amongst T cells in the presence or absence of peptide stimulation, and varied in mobile vs. stationary T cells[20]. Therefore, whilst the magnitude of changes in intracellular calcium concentration is an important arbiter of T cell effector potential, the 'rhythm' of these responses may yet yield valuable information that has been under-investigated. This is in no small part because of the requirement for real-time analyses of individual responding T cells and the technical complexities associated with this approach. Our solution to this problem utilises a platform with the capacity to capture and activate T cells and present them for real-time analyses of intracellular calcium flux over time. Furthermore, algorithms developed to analyse images of these fluxing cells can clearly differentiate between those which have been strongly or weakly stimulated. We believe that this provides a new way to measure T cell responses and T cell response potential, in real-time and on an individual cell basis.

Results

Solid-state platforms can detect activation in T cells stimulated by lower affinity ligands compared to bulk population analysis. Our platform uses plasma polymerisation to immobilise ligands on material surfaces to capture and activate $CD3^+$ T cells causing intracellular calcium flux and has been previously validated[21,22,23] (shown schematically in Supplementary Fig. S1). To determine whether this platform could be used to differentiate the strength of $CD3^+$-mediated T cell activation based on the changes in the observed patterns of calcium flux, we compared whole bivalent antibody (anti-CD3) and lower avidity fragmented variants (anti-$CD3_{(Fab)}$), with and without CD28 co-stimulation. Activation of naïve T cells using anti-CD3 ± anti-CD28 generated a steady increase in fluorescence when detected using flow cytometry (Fig. 1a(i) and b(i)) or averaged from individual cell fluorescence collected by confocal microscopy (Fig. 1a(ii) and b(ii)). To equivalently represent a 'population' of cells between flow cytometry and confocal microscopy, both 'responding' and 'non-responding' cells were graphed in the latter, to demonstrate the tracking of individual cells for assessing response potential and capacity. The use of solid-state platforms for this purpose is advantageous over flow cytometry whereby responding cells may be lost due to its 'snap-shot' nature of detection. The results from these analyses suggest that when T cells respond to high affinity bivalent antibodies, irrespective of co-stimulation, the sum of calcium flux patterns elicited in response to platform-immobilised antibodies is comparable to the response profiles of a bulk population stimulated with soluble ligands and analysed by flow cytometry.

To further investigate the role of CD28 co-stimulation, we 'sensitised' the T cells prior to anti-CD3 exposure, which has been shown to augment calcium responses through independent ERK signalling[23]. When naïve T cells were stimulated in this manner, there was a similar increase in calcium flux detected by flow cytometry (Fig. 1c(i)). The combined average of individual cells (Fig. 1c(ii)) had a slightly higher release of calcium between 180–500 seconds, but followed the similar pattern previously seen with anti-CD3 ± anti-CD28 (Fig. 1a(ii) and b(ii)). In comparing the responses elicited by soluble and immobilised low avidity anti-$CD3_{(Fab)}$, with and without CD28 co-simulation, an increase in the calcium signal was evident only when individual cells were analysed (Fig. 1d(ii) and e(ii)) and not in whole populations (Fig. 1d(i) and e(i)). Interestingly, the anti-CD28-sensitised T cells did not exhibit an increase in calcium flux (Fig. 1f(i) and (ii)) as was seen with anti-CD3-coated surfaces (Fig. 1c(ii)). This may suggest stoichiometric limitations of anti-$CD3_{(Fab)}$ interactions when there are additional proteins bound onto a single cell. However, even with additional CD28 co-stimulation, the signal elicited by immobilised anti-$CD3_{(Fab)}$ was weaker than that seen with immobilised bivalent anti-CD3 (Fig. 1d(ii) and e(ii), compared to, a(ii)). Notwithstanding contributions from anti-CD28, it was evident that soluble anti-$CD3_{(Fab)}$ failed to elicit any response from T cells when analysed by flow cytometry (Fig. 1d–f(i)). These results allow for a distinction to be made between platform-immobilised low avidity monovalent antibodies, where calcium responses were still detectable, and the same antibodies in solution, where regardless of co-stimulation, no T cell responses could be detected. Interestingly, calcium responses were detected on the platform to both forms of anti-CD28 co-stimulation either immobilised (adh) (Fig. 1g(ii)) or sensitised (sens) prior to activation (Fig. 1h(ii)). Whilst these increases were moderate, T cell signalling through CD28 or cross-linking of anti-CD28 may result indirectly in intracellular calcium increases, as previous studies have demonstrated anti-CD28 alone can upregulate proximal proteins in T cell activation signalling upstream of calcium flux[24–26]. Importantly, these results highlight the limitation of using flow cytometry for detecting weak TCR interactions, whereas two dimensional platforms enable planar cell binding and facilitate detection of calcium responses. Hence, these results also provide a defined suite of ligands that display decreasing ability to stimulate T cells in the following order: immobilised anti-CD3 + anti-CD28 (sens) > anti-CD3 ± anti-CD28 > anti-$CD3_{(Fab)}$ + anti-CD28 > anti-$CD3_{(Fab)}$. Consequently, we show that the patterns of calcium flux correlate with T cell signalling strength.

The strength of TCR stimulation affects the rate of calcium oscillations. To this end, algorithms to quantify gross changes in the calcium release (oscillations) were developed using a Haarlet transformation (Supplementary Fig. S2, and described in the 'Methods' section). The use of a threshold allowed the detection of frequencies of 'threshold crossings', correlating to large spikes in calcium concentration as seen by increases in the fluorescence ratio (Supplementary Fig. S2). Individual cells displaying heterogeneous responses (Fig. 2a) were similarly analysed, and the corresponding time to first oscillation (Fig. 2b) was further plotted as an empirical cumulative distribution function (ECDF).

Assessment of the total population (responders and non-responders) revealed that a stronger ligand-receptor interaction was able to enhance the rate of calcium release (Fig. 3a). There was a significant increase in the rate of calcium release between anti-CD3 and its anti-$CD3_{(Fab)}$ counterpart as determined through Cox regression analysis ($p = 2.77 \times 10^{-28}$), with a four-fold increased probability of a faster time to first oscillation (Supplementary Table S2). However, no statistical differences were observed with the addition of co-stimulation (Supplementary Fig. S3). The calcium rates for anti-$CD3_{(Fab)}$ + anti-CD28(sens) T cells were shown to be significantly reduced ($p = 0.0064$) compared to anti-CD28(sens) alone resulting from nonspecific cross-linking on streptavidin surfaces (Supplementary Fig. S4). As observed for the population analysis (Fig. 1f), the hindrance of multi-protein interactions may have limited subsequent analyses of the anti-$CD3_{(Fab)}$ + anti-CD28(sens) data sets. Unexpectedly, the time to first oscillation for anti-CD28 sensitised, anti-CD3 activated T cells were significantly reduced in comparison to co-stimulation with immobilised anti-CD28 or anti-CD3 alone ($p = 1.36 \times 10^{-5}$ and $p = 1.74 \times 10^{-9}$, respectively).

To evaluate whether the changes were directly attributed to the proportion of responding cells, or rather, an intrinsic ability to 'sense' ligands, the responding population alone was subjected to the analysis (Fig. 3b). Similarly, we observed a statistical increase in calcium release amongst anti-CD3 vs anti-$CD3_{(Fab)}$ stimulation with or without anti-CD28 ($p = 1.03 \times 10^{-3}$ and $p = 9.84 \times 10^{-3}$, respectively). We also observed that CD28 co-stimulation slightly increased the rate of calcium release for anti-$CD3_{(Fab)}$, however this was not sig-

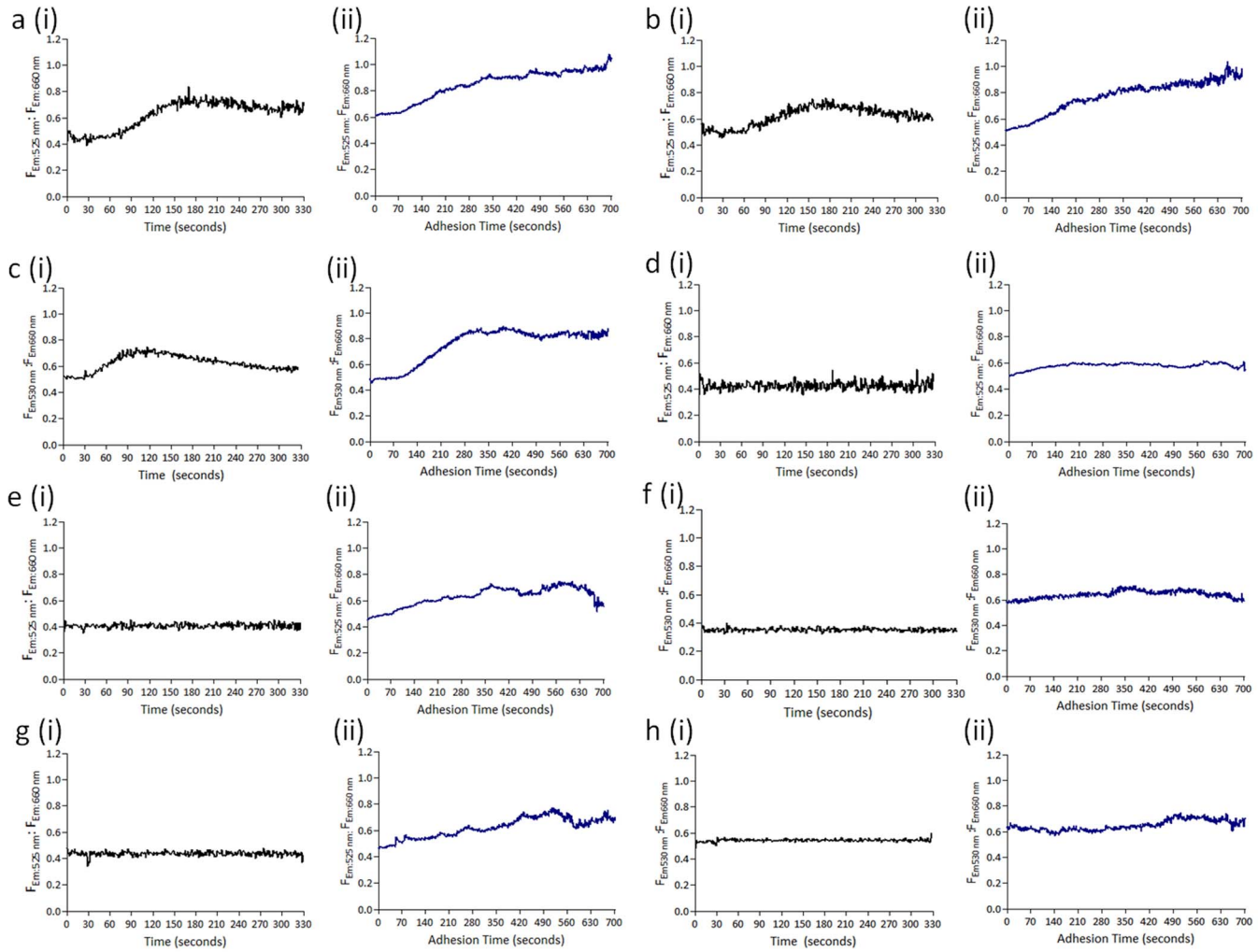

Figure 1 | Functionalised material surfaces can effectively activate T cells to calcium flux. Calcium flux was detected in naive T cells probed with Fluo-4 AM ($F_{Em:525\ nm}$) and Fura Red AM ($F_{Em:660\ nm}$) upon stimulation with (a) anti-CD3, (b) anti-CD3 + anti-CD28, (c) anti-CD3 + anti-CD28(sensitised), (d) anti-$CD3_{(Fab)}$, (e) anti-$CD3_{(Fab)}$ + anti-CD28, (f) anti-$CD3_{(Fab)}$ + anti-CD28(sensitised), (g) anti-CD28, or (h) anti-CD28(sensitised) ligands by flow cytometry (i) or confocal microscopy (ii). (i) T cells were labelled with anti-CD3, anti-CD3 + anti-CD28, anti-$CD3_{(Fab)}$, or anti-$CD3_{(Fab)}$ + anti-CD28, biotinylated ligands. In some cases, T cells were sensitised with purified hamster anti-mouse CD28 followed by cross-linking with anti-hamster IgG. Baseline fluorescence was recorded for 30 seconds before the addition of streptavidin, and fluorescence was measured for an additional 300 seconds. (ii) Fluorescence was recorded every second using confocal microscopy, and the $F_{Em:525\ nm}$ to $F_{Em:660\ nm}$ ratio calculated for individual cells using Fiji software. The following numbers are expressed as n = number of individual cells collected [responding cells]; (a) n = 250 [175], (b) n = 208 [128], (c) n = 209 [78], (d) n = 425 [148], (e) n = 300 [106], (f) n = 57 [21], (g) n = 210 [54] and (h) n = 112 [28], which were combined to generate a population average.

nificant ($p = 0.67$). Anti-CD3 + anti-CD28(sens) T cells appeared to have a profile more similar to anti-CD3 ± anti-CD28(adh), however the oscillatory response was marginally reduced ($p = 0.04092$). It is interesting to note differences in the individual calcium traces observed by several representative cells (Fig. 4). Whilst there were cells that follow similar patterns to anti-CD3 traces, there were also cells that exhibited lower oscillatory potential, but appeared to maintain a more consistent and higher calcium concentration. This could be interpreted to mean that T cells that have a more robust stimulation do not require frequent oscillations to reach a threshold of calcium signalling to proceed.

To further investigate oscillation frequency, we analysed the time between first and second oscillation, which revealed less variance between different TCR ligands at early time points (Fig. 3c). The overall calcium rate in anti-CD3 stimulated cells remained statistically greater as compared to anti-$CD3_{(Fab)}$ ($p = 0.0055$). Interestingly, it appeared an equal proportion of the populations for all stimulation conditions followed a similar rate between the first and second oscillation. However, distinct divergences were seen around 100–110 seconds, and earlier for anti-$CD3_{(Fab)}$ ± anti-CD28(adh). The rate for anti-CD3 + anti-CD28(sens) was significantly decreased as compared to anti-CD3 ($p = 0.0219$) with a relative risk (ratio of the probability of first oscillations between stimulations) of 1.45, in favour of a faster calcium response for anti-CD3 (Supplementary Fig. S3). The overlapping graphs for anti-$CD3_{(Fab)}$ ± anti-CD28(adh) is in contrast to the differences observed for the time to first oscillation, and surprisingly, appear to follow a similar trend to anti-CD3 + anti-CD28(sens). Whilst the algorithm limits the ability to mechanistically explain reduced oscillatory potential, it is important to make note of the magnitude of the response, evidently expressed at both the population level (Figure 1c–e(ii)) and individual cell level (Fig. 4). When compared with anti-CD3, anti-CD3 + anti-CD28(sens) had moderately, but significantly, reduced time to first oscillation and time between first and second oscillation. Nonetheless, the consistently disparate curves for divalent vs monovalent binding indicates the original

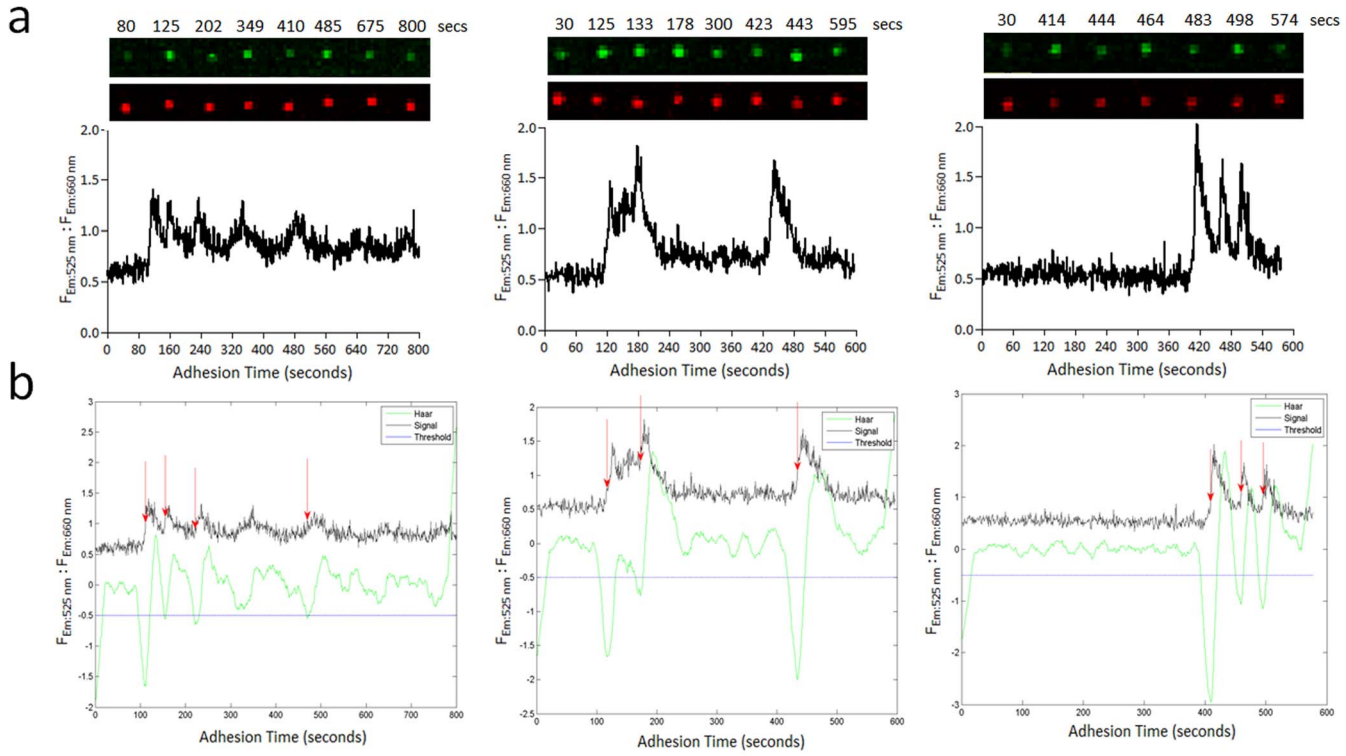

Figure 2 | Example of heterogeneous calcium patterns of individual responding cells activated on material surfaces functionalised with anti-CD3$_{(Fab)}$ + anti-CD28. (a) Three examples are shown here, with individual fluorescence channels highlighting the simultaneous increase and decrease in $F_{Em:525\ nm}$ (green) and $F_{Em:660\ nm}$ (red), respectively. (b) Wavelet transformations were applied to individual calcium graphs to quantify threshold crossings

TCR interaction can modulate the rate of calcium signalling as determined through single cell analysis.

Discussion

Our results demonstrate that there are distinct patterns in the magnitude and rhythm of calcium flux oscillations in T cells directly relating to the strength of stimulus. The rate of calcium flux was consistently higher in stronger bivalent antibody stimulation compared to its monovalent Fab counterpart. Interestingly, the addition of anti-CD28 co-stimulation reduced oscillatory potential but demonstrated a sustained calcium flux. Material surfaces functionalised with a suite of anti-CD3 variants were shown to capture and activate T cells as seen by the increase in intracellular calcium concentration. We observed that the sum of individual calcium flux patterns elicited in response to platform-immobilised bivalent antibodies was comparable to the response profiles of a bulk population stimulated with soluble ligands. The results also demonstrated that calcium responses by low avidity stimulation were only detected when monovalent ligands (anti-CD3$_{(Fab)}$ ± anti-CD28) were immobilised onto the platform and not measurable in solution using flow cytometry. Although flow cytometry is the standard method of calcium detection, it is evident that the 'snap-shot' nature of bulk analysis masks interpretable and valuable response heterogeneity[5,7,27].

Consistent with previous studies, single T cells displayed a broad spectrum of calcium patterns with varying frequency and magnitude of oscillations. The classification of responses based on these parameters are widely reported, however the ability to reach that initial oscillation is a striking and deliberate effort by the T cell. For this reason we developed automated algorithms that could quantify the time to first oscillation upon cell adhesion on the stimulating platform. Importantly, the large numbers of cells collected are ideal for statistical comparisons and exceed the data currently reported in the literature. When directly comparing bivalent and monovalent ligands (anti-CD3 vs anti-CD3$_{(Fab)}$), it was not surprising to observe that higher TCR binding affinity demonstrated a faster time to first oscillation in the total population, and in the responding population, which was also analysed to negate the directly confounding effect of different proportions of responders (70% vs 35%, respectively). Therefore, when analysing the responding population only (Fig. 3b), it was evident that the rate of calcium release was a function of both binding strength and the number of T cells contributing to the response. Equivalent human anti-CD3$_{(Fab)}$ ligands have shown an affinity constant that is two-three times weaker than that of divalent anti-CD3[28]. The ability to stimulate T cells with anti-CD3$_{(Fab)}$ is considered poor[29,30], however binding is sufficient to induce TCR conformational changes[30,31] that result in the activation of proximal T cell signalling molecules[28,31–33], oscillatory calcium signals[33], and IL-2 production *in vitro*[33,34] but minimal cytokine responses *in vivo*[35]. Akin to these observations, physiological manipulation of ligand affinity through altered peptide ligands have demonstrated that higher affinity ligands allow for 'full' T cell activation through optimal TCR interaction[36–38]. Therefore, the delay and reduced magnitude of calcium responses by weak ligands is a product of binding conditions that generate suboptimal signalling pathways upstream of calcium flux[39–41].

However, given these results, it was expected that anti-CD28 co-stimulation would increase the calcium response through enhancing signalling pathways as well as strengthening the affinity between the T cell and the platform. In the case of adherent anti-CD28, we were surprised to find no significant difference in calcium responses when stimulated with anti-CD3 ligands (whole antibody or Fab). This result however could be attributed to suboptimal binding ratios between the two ligands on the platform surfaces. Therefore, we explored a recently described method of sensitising T cells prior to activation. Byrum et al (2013) demonstrated that cross-linking anti-CD28 on Jurkat T cells potentiates the calcium response upon anti-

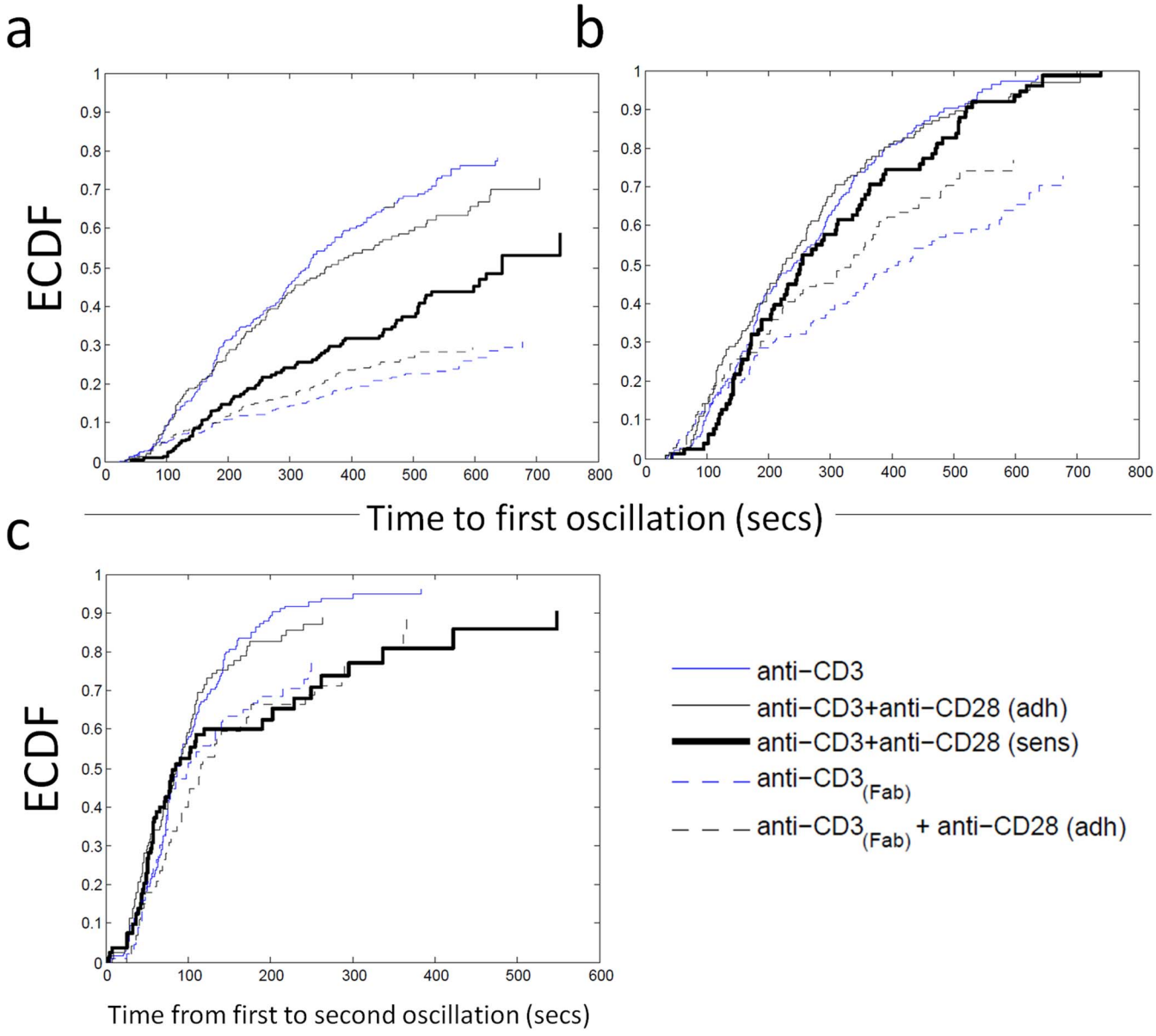

Figure 3 | Quantifying calcium flux patterns within individual responding T cells. The empirical cumulative distribution function (ECDF) for the time to first calcium oscillation was analysed for anti-CD3 (solid blue line), anti-CD3 + antiCD28(adh) (solid black line), anti-CD3 + anti-CD28(sens) (thick solid black line), anti-$CD3_{(Fab)}$ (dotted blue line) and $CD3_{(Fab)}$ + anti-CD28(adh) (dotted black line) for the total population (a) and the responding population only (b). The time between first and second oscillation was further analysed (c).

CD3 activation in an ERK-dependent manner[24]. Unexpectedly, we did not observe a substantial increase in the response magnitude of the overall population when T cells were sensitised with anti-CD28 co-stimulation prior to anti-CD3 activation (Fig. 1c(i)). However, single cell analysis revealed a slower time to first and second oscillation (anti-CD3 ± anti-CD28(sens), Fig. 3b and c), indicative of reduced oscillatory potential and a more sustained calcium response (Fig. 4). This is in accordance with numerous studies that demonstrate weaker ligands utilise oscillatory patterns to enhance efficiency for crossing the activation threshold[27,42]. Interestingly, the pattern of oscillations has shown to differentially control NFAT and NFκβ transcription factors that regulate cytokine production[18,19,43–45]. NFκβ is more sensitive to infrequent oscillations when compared to NFAT, which requires sustained calcium signals to prevent phosphorylation and translocation from the nucleus[43,46].

One possible explanation for differential calcium kinetics as a function of TCR ligand binding is taken from observations of a study by Chen et al (2010) that demonstrated the initial spike is a result of ER store release, and the subsequent signals result from influx through CRAC channels via SOCE[47]. Furthermore, it has been established that the capacity of influx is directly proportional to the ER store depletion, a model that forms the basis of SOCE[48–50]. The linearity of the capacity to deplete ER calcium stores to determine the subsequent degree and timing of influx may offer an explanation for oscillatory vs sustained patterns in weak and strong ligands, respectively. Based on our observations and that of others[24], we propose the hypothesis that anti-CD28 sensitised T cells induce partial or full ER store depletion of calcium ions, which causes partial ERK activation, thereby 'priming' the T cell for a more robust and sustained influx upon TCR stimulation, subsequently enhancing the recruitment of downstream effectors. This is also validated by several lines of observations; (1) previous studies have demonstrated anti-CD28 alone can up-regulate proximal proteins in T cell activation signalling upstream of calcium flux[24–26], (2) platform immobilised anti-CD28

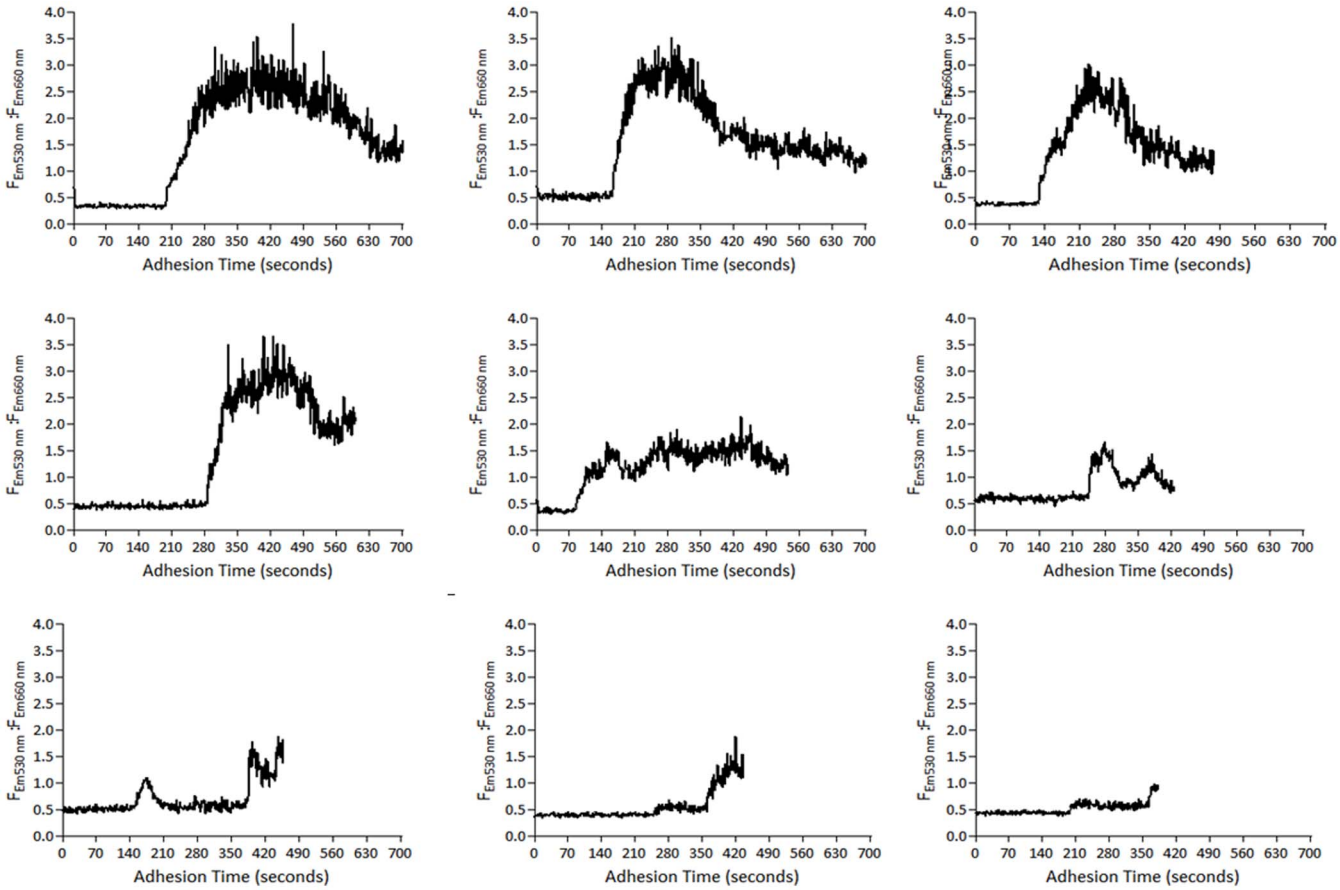

Figure 4 | Individual calcium traces for T cells sensitised to anti-CD28 prior to activation on anti-CD3 immobilised surfaces. The calcium traces of nine representative were plotted, whereby differences in adhesion time are attributed to various times of deposition onto the surface between cell addition (t = 0 secs) to the end of recording (t = 800 secs).

alone could induce detectable calcium responses in our hands (Fig. 1g(ii)), (3) the distal activation of ERK in T cells[24] appears to be calcium-dependent through the balance of Ras GEF and GAP functionality[51], and (4) unpulsed target cells have the capacity to cause weak influx in conjugated T cells[52,53], however this is insufficient for activation[52]. Assessment of ER depletion mechanisms would also warrant the study of proteins involved, namely STIM1 and Orai1. It would be interesting to assess the involvement, if any, of 'distal caps' in this system to gain an understanding of how differential TCR signalling can directly affect cap formation and subsequent influx[12]. Nevertheless, further investigation is required to confirm and detail the molecular pathways activated upon anti-CD28 binding alone, as well as deducing the resultant calcium flux patterns when co-stimulation is received prior to, or in conjugation with TCR signals.

This study in summary describes a novel algorithm for detecting the rate of calcium flux in activated T cells. The calcium flux of individual T cells revealed heterogeneous patterns, represented by various rhythms or 'oscillations'. These data sets were used to generate a computational algorithm to plot the rate of calcium release to first and second oscillations over time, a process which cannot be reproduced for bulk-analysed flow cytometric data. This method therefore presents an assay for assessing calcium flux that is amenable to altered activation parameters as demonstrated here with bivalent antibody and monovalent Fab fragments binding the TCR. The data highlight that stronger primary stimulation can result in significantly faster times to first and second oscillations and a greater magnitude of calcium flux.

Methods

Plasma polymerisation. Gas plasma polymerisation was conducted using a custom-built plasma unit driven by a 13.56 MHz power generator with a matching network. Propanal (propionaldehyde, >99% purity; Sigma) was used as the process gas to deposit a plasma polymer layer of aldehyde groups approximately 30 nm thick onto a microscope slide (operating pressure of 0.21 mbar, 40 W input power, and process time of one minute). Slides were then cleaned with ethanol, rinsed with MilliQ water, and dried with filtered nitrogen gas.

Animals. Six to ten week old C57Bl/6 mice were used in this study, and were housed at the Reid Animal Facility, University of South Australia (Adelaide). All experimental protocols were approved by the Animal Ethics Committees of SA Pathology (Project Number 113/10) and the University of Adelaide (Project Number M204/11). All methods were performed in accordance to the guidelines of the University of South Australia (South Australian Animal Welfare Act 1985). The obtain naïve T cells, lymph nodes were harvested and a single cell suspension prepared. Naïve T cells were maintained at 37°C (5% CO2 and air) in complete RPMI (Gibco) supplemented with 10% heat-inactivated foetal calf serum, 100 U/ml penicillin, 100 ug/ml gentamycin, 2 mM B-mercaptoethanol (2 mM), 2 mM L-glutamine and 10 mM HEPES.

Generating anti-CD3$_{(Fab)}$ fragments. The anti-CD3$_{(Fab)}$ fragments were prepared as previously described[54]. Briefly, anti-CD3ε antibody was purified from supernatants of cultured 145-2C11 hybridomas on a protein G-sepharose column using affinity chromatography. The antibody solution was concentrated on a 30,000 MWCO spin column (Merck Millipore), and stored in PBS. To fragment the whole antibody, no greater than five milligrams was digested at one time with a papain solution (Sigma) for eight hours before being stopped with 0.03 M iodoacetamide (Sigma). Fragmented antibody solution was run on a protein A-sepharose column several times to remove Fc antibody fragments, and further purified using 30, 000 and 100, 000 MWCO spin columns. The anti-CD3$_{(Fab)}$ solutions were regularly checked with coomassie staining of SDS-PAGE gels. The anti-CD3$_{(Fab)}$ ligands were then biotinylated using the EZ-Link Sulfo-NHS-Biotin kit (Thermo Scientific) as per manufacturer's instructions, and verified by western blot.

Preparing functionalised material surfaces. Twelve-well flexiPERM culture masks (Greiner Bio-one) were fixed to the plasma polymerised slides and incubated with streptavidin (Sigma; 5 μg/ml, 4°C, overnight). Wells were then washed (seven times, 1 × PBS), blocked (0.01% BSA, 30 mins) and washed again (seven times, 1 × PBS). Saturating levels of biotinylated ligands were incubated on streptavidin-coated surfaces for 90 mins at room temperature, and washed seven times with 1 × PBS. The biotinylated ligands included anti-CD3 (5 μg/ml, clone 145-2C11; eBioscience), anti-CD28 (2.5 μg/ml, clone 37.51; eBioscience) and anti-$CD3_{(Fab)}$ (1/50 dilution, clone 145-2C11; as prepared above).

Probing intracellular calcium. For ratiometric detection of intracellular calcium flux, naive T cells (3×10^6) were stained with 4 μM Fluo-4 AM (Molecular Probes), 10 μg/ml Fura Red AM (Molecular Probes) and 0.02% Pluronic F-127 (AAT Bioquest) in HBSS for 30 mins at 37°C with gentle agitation. Following one wash in HEPES buffered saline (HBS) solution, the cells were resuspended at 1×10^6 cells/ml and incubated for 45 mins at room temperature to allow sufficient cleavage of AM esters rendering the probes cell impermeable. The cells required for flow cytometry experiments were subsequently incubated with anti-CD3-biotin and or anti-CD28-biotin (10 μg/ml; 20 mins, room temperature), washed (three times, HBS) and resuspended at 1×10^6 cells/ml. All cells were maintained at 37°C until required.

Anti-CD28 sensitisation prior to T cell stimulation. Naïve T cells were sensitised to anti-CD28 signalling prior to anti-CD3 activation, as previously described[23]. Briefly, probe-loaded T cells were resuspended in 100 μl of 1 × PBS and incubated with 7.5 μg of purified hamster anti-mouse CD28 for 45 mins on ice. Purified anti-hamster IgG was incubated for an additional 30 mins on ice, before the cells were washed and resuspended at 1×10^6 cells/ml in HBS.

Flow cytometric detection of calcium flux. Intracellular calcium flux was detected using the FACSCanto II flow cytometer (BD Bioscience). Fluorescent probes were excited with a single 488 nm excitation laser, and emission collected in the 530/30 nm filter for Fluo-4 AM and 670 nm filter for Fura Red AM. The ratio of Fluo-4 AM ($F_{Em:525\ nm}$) and Fura Red AM ($F_{Em:660\ nm}$) fluorescence was used to detect changes in calcium concentration as a function of fluorescence intensity. Baseline fluorescence of antibody-bound naive T cells (2×10^5) was measured for 30 seconds before the addition of streptavidin (final concentration of 1 μg/ml) to induce T cell receptor cross linking and T cell activation. Data was collected using the FACSDiva v6.1.3 software (BD Bioscience) and FlowJo 7.6.4 software (Tree Star) was used for analysis of mean fluorescence over time.

Confocal imaging acquisition and ratiometric calcium analysis for single cells. The Bio-Rad Radiance 2100 confocal microscope was used to collect time lapse images of naive T cells activated on ligand-functionalised surfaces. The calcium probe-loaded T cells were added to the well of interest, and immediately focused to allow accurate fluorescence detection. The cells were then excited with an Argon 488 nm laser, and emission viewed through a HQ515/30 nm narrow band filter for Fluo-4 AM and 660 nm long pass filter for Fura Red AM. The transmission detector was used to visualise moving cells, with transmission and fluorescence images simultaneously collected and automatically merged. Images were taken using a 20 × long working distance objective lens (NA 0.7) at one second intervals for a total of 800 images. Data was analysed using Fiji (Image J, NIH) by selecting individual cell regions with appropriate gating tools, then plotting mean fluorescence over time for each fluorescent channel (Fluo-4 AM, $F_{Em:660\ nm}$; Fura Red AM, $F_{Em:660\ nm}$) exclusively for the selected region. Stringent criteria were used to assess fluorescence changes as a function of calcium flux (Supplementary Table S1). Microsoft Excel was used to calculate the Fluo-4 AM to Fura Red AM ratio for individual cells, and the resulting data was graphed using GraphPad Prism v5.

Computational analysis of single cells. Software for calcium oscillations detection and statistical analysis were written in Matlab™. A numerical approach provided a consistent method to identify calcium transients. The calcium signal was filtered with the wavelet transform using a Haar basis function. The Haar Wavelet transformation is a mathematical technique that is used to transform signals of a time series into a 'wavelet' formulation. The Haar wavelet is a form of signal processing with an orthonormal system, which means the information of the original signal is preserved in the transformed data and simply offers an alternative representation of the same mathematic entity. The information to be gained in Haar transformations are: (1) the frequency spectrum, which show the frequencies that exist (i.e., oscillations), and (2) the location information, which details the instants (ie, time) when a change in frequency occurs. Using this method, a wavelet scale factor of 40 was selected to reject high frequency noise and low frequency baseline variations (Supplementary Fig. S2). Local minima of the transformed data corresponded to the upstroke of calcium spikes (green trace, Supplementary Fig. S2). A threshold crossing value of −0.5 was used to identify the time intervals used to find local minima. The empirical cumulative distribution function (ECDF) for the time to the first spike was calculated with right censoring (no spike detected during the period of observation). The time-dependence and large sample size of the data advocates the use of ECDF as an effective plot, which in the case of survival, is equivalent to the expression of data seen on a Kaplan-Meier or survival curve. Therefore, over a time domain, the accumulated proportions of cells that have achieved a first oscillation are plotted. Statistical analysis was performed using cox regression to determine if the various stimulation groups influenced the time to the first calcium spike.

1. Gerlach, C. *et al.* Heterogeneous differentiation patterns of individual CD8+ T cells. *Science.* **340**, 635–639 (2013).
2. Lopez, J. A. *et al.* Rapid and unidirectional perforin pore delivery at the cytotoxic immune synapse. *J Immunol.* **191**, 2328–2334 (2013).
3. Camisaschi, C. *et al.* Effects of cyclophosphamide and IL-2 on regulatory CD4+ T cell frequency and function in melanoma patients vaccinated with HLA-class I peptides: impact on the antigen-specific T cell response. *Cancer Immunol Immunother.* **62**, 897–908 (2013).
4. Xu, W. *et al.* The nucleocapsid protein of Rift Valley fever virus is a potent human CD8+ T cell antigen and elicits memory responses. *PLoS One* **8**, e59210 (2013).
5. Wu, S., Jin, L., Vence, L. & Radvanyi, L. G. Development and application of 'phosphoflow' as a tool for immunomonitoring. *Expert Rev Vaccines* **9**, 631–643 (2010).
6. Chen, D. S. *et al.* Marked differences in human melanoma antigen-specific T cell responsiveness after vaccination using a functional microarray. *PLoS Med.* **2**, e265 (2005).
7. Salles, A. *et al.* Barcoding T cell calcium response diversity with methods for automated and accurate analysis of cell signals (MAAACS). *PLoS Comput Biol.* **9**, e1003245 (2013).
8. Lewis, R. S. Calcium signaling mechanisms in T lymphocytes. *Annu Rev Immunol.* **19**, 497–521 (2001).
9. Oh-hora, M. & Rao, A. Calcium signaling in lymphocytes. *Curr Opin Immunol.* **20**, 250–258 (2008).
10. Liou, J. *et al.* STIM is a Ca2+ sensor essential for Ca2+-store-depletion-triggered Ca2+ influx. *Curr Biol.* **15**, 1235–1241 (2005).
11. Prakriya, M. *et al.* Orai1 is an essential pore subunit of the CRAC channel. *Nature* **443**, 230–233 (2006).
12. Barr, V. A. *et al.* Dynamic movement of the calcium sensor STIM1 and the calcium channel Orai1 in activated T-cells: puncta and distal caps. *Mol Biol Cell.* **19**, 2802–2817 (2008).
13. Feske, S., Skolnik, E. Y. & Prakriya, M. Ion channels and transporters in lymphocyte function and immunity. *Nat Rev Immunol.* **12**, 532–547 (2012).
14. Guse, A. H., Berg, I., da Silva, C. P., Potter, B. V. & Mayr, G. W. Ca2+ entry induced by cyclic ADP-ribose in intact T-lymphocytes. *J Biol Chem.* **272**, 8546–8550 (1997).
15. Guse, A. H., Roth, E. & Emmrich, F. Intracellular Ca2+ pools in Jurkat T-lymphocytes. *Biochem J.* **291 (Pt 2)**, 447–451 (1993).
16. Dupont, G., Combettes, L., Bird, G. S. & Putney, J. W. Calcium oscillations. *Cold Spring Harb Perspect Biol.* **3**, a004226 (2011).
17. Joseph, N., Reicher, B. & Barda-Saad, M. The calcium feedback loop and T cell activation: how cytoskeleton networks control intracellular calcium flux. *Biochim Biophys Acta.* **1838**, 557–568 (2014).
18. Dolmetsch, R. E., Xu, K. & Lewis, R. S. Calcium oscillations increase the efficiency and specificity of gene expression. *Nature.* **392**, 933–936 (1998).
19. Tomida, T., Hirose, K., Takizawa, A., Shibasaki, F. & Iino, M. NFAT functions as a working memory of Ca2+ signals in decoding Ca2+ oscillation. *EMBO Journal* **22**, 3825–3832 (2003).
20. Mues, M. *et al.* Real-time in vivo analysis of T cell activation in the central nervous system using a genetically encoded calcium indicator. *Nat Med.* **19**, 778–783 (2013).
21. Coad, B. R. *et al.* Immobilized streptavidin gradients as bioconjugation platforms. *Langmuir.* **28**, 2710–2717 (2012).
22. Diener, K. R. *et al.* Solid-state capture and real-time analysis of individual T cell activation via self-assembly of binding multimeric proteins on functionalized materials surfaces. *Acta Biomater.* **8**, 99–107 (2012).
23. Christo, S. N. *et al.* Individual and population quantitative analyses of calcium flux in T-cells activated on functionalized material surfaces. *Aust J Chem.* **65**, 45–49 (2012).
24. Byrum, J. N., Van Komen, J. S. & Rodgers, W. CD28 sensitizes TCR Ca(2)(+) signaling during Ag-independent polarization of plasma membrane rafts. *J Immunol.* **191**, 3073–3081 (2013).
25. Kovacs, B. *et al.* Ligation of CD28 by its natural ligand CD86 in the absence of TCR stimulation induces lipid raft polarization in human CD4 T cells. *J Immunol.* **175**, 7848–7854 (2005).
26. Miller, J. *et al.* Two pathways of costimulation through CD28. *Immunol Res.* **45**, 159–172 (2009).
27. Kupzig, S., Walker, S. A. & Cullen, P. J. The frequencies of calcium oscillations are optimized for efficient calcium-mediated activation of Ras and the ERK/MAPK cascade. *Proc Natl Acad Sci U S A.* **102**, 7577–7582 (2005).
28. Kjer-Nielsen, L. *et al.* Crystal structure of the human T cell receptor CD3 epsilon gamma heterodimer complexed to the therapeutic mAb OKT3. *Proc Natl Acad Sci U. S. A.* **101**, 7675–7680 (2004).
29. Risueno, R. M., Schamel, W. W. & Alarcon, B. T cell receptor engagement triggers its CD3epsilon and CD3zeta subunits to adopt a compact, locked conformation. *PLoS One* **3**, e1747 (2008).
30. Kim, S. T. *et al.* The alphabeta T cell receptor is an anisotropic mechanosensor. *J Biol Chem.* **284**, 31028–31037 (2009).

31. Gil, D., Schamel, W. W., Montoya, M., Sanchez-Madrid, F. & Alarcon, B. Recruitment of Nck by CD3 epsilon reveals a ligand-induced conformational change essential for T cell receptor signaling and synapse formation. *Cell* **109**, 901–912 (2002).
32. Rojo, J. M., Bello, R. & Portoles, P. T-cell receptor. *Adv Exp Med Biol.* **640**, 1–11 (2008).
33. Tamura, T. *et al.* Molecular mechanism of the impairment in activation signal transduction in CD4(+) T cells from old mice. *Int Immunol.* **12**, 1205–1215 (2000).
34. Tamura, T. & Nariuchi, H. T cell activation through TCR/-CD3 complex. IL-2 production of T cell clones stimulated with anti-CD3 without cross-linkage. *J Immunol.* **148**, 2370–2377 (1992).
35. Malcolm, S. L., Smith, E. L., Bourne, T. & Shaw, S. A humanised mouse model of cytokine release: comparison of CD3-specific antibody fragments. *J Immunol Methods* **384**, 33–42 (2012).
36. Evavold, B. D., Sloan-Lancaster, J. & Allen, P. M. Tickling the TCR: selective T-cell functions stimulated by altered peptide ligands. *Immunol Today* **14**, 602–609 (1993).
37. Sloan-Lancaster, J. & Allen, P. M. Altered peptide ligand-induced partial T cell activation: molecular mechanisms and role in T cell biology. *Annu Rev Immunol.* **14**, 1–27 (1996).
38. Rabinowitz, J. D. *et al.* Altered T cell receptor ligands trigger a subset of early T cell signals. *Immunity* **5**, 125–135 (1996).
39. Reis e Sousa, C., Levine, E. H. & Germain, R. N. Partial signaling by CD8+ T cells in response to antagonist ligands. *J Exp Med.* **184**, 149–157 (1996).
40. Sloan-Lancaster, J., Shaw, A. S., Rothbard, J. B. & Allen, P. M. Partial T cell signaling: altered phospho-zeta and lack of zap70 recruitment in APL-induced T cell anergy. *Cell* **79**, 913–922 (1994).
41. Madrenas, J. *et al.* Zeta phosphorylation without ZAP-70 activation induced by TCR antagonists or partial agonists. *Science* **267**, 515–518 (1995).
42. Chen, Y. Z., Lai, Z. F., Nishi, K. & Nishimura, Y. Modulation of calcium responses by altered peptide ligands in a human T cell clone. *Eur J Immunol.* **28**, 3929–3939 (1998).
43. Dolmetsch, R. E., Lewis, R. S., Goodnow, C. C. & Healy, J. I. Differential activation of transcription factors induced by Ca2+ response amplitude and duration. *Nature* **386**, 855–858 (1997).
44. Li, W., Llopis, J., Whitney, M., Zlokarnik, G. & Tsien, R. Y. Cell-permeant caged InsP3 ester shows that Ca2+ spike frequency can optimize gene expression. *Nature* **392**, 936–941 (1998).
45. Zhu, L. *et al.* Ca2+ oscillation frequency regulates agonist-stimulated gene expression in vascular endothelial cells. *J Cell Sci.* **121**, 2511–2518 (2008).
46. Hu, Q., Deshpande, S., Irani, K. & Ziegelstein, R. C. [Ca(2+)](i) oscillation frequency regulates agonist-stimulated NF-kappaB transcriptional activity. *J Biol Chem.* **274**, 33995–33998 (1999).
47. Chen, J. L. *et al.* Ca2+ release from the endoplasmic reticulum of NY-ESO-1-specific T cells is modulated by the affinity of TCR and by the use of the CD8 coreceptor. *J Immunol.* **184**, 1829–1839 (2010).
48. Dolmetsch, R. E. & Lewis, R. S. Signaling between intracellular Ca2+ stores and depletion-activated Ca2+ channels generates [Ca2+] i oscillations in T lymphocytes. *J Gen Physiol.* **103**, 365–388 (1994).
49. Donnadieu, E., Bismuth, G. & Trautmann, A. Calcium fluxes in T lymphocytes. *J Biol Chem.* **267**, 25864–25872 (1992).
50. Zweifach, A. & Lewis, R. S. Calcium-dependent potentiation of store-operated calcium channels in T lymphocytes. *J Gen Physiol.* **107**, 597–610 (1996).
51. Muallem, S. Decoding Ca2+ signals: a question of timing. *J Cell Biol.* **170**, 173–175 (2005).
52. Faroudi, M. *et al.* Lytic versus stimulatory synapse in cytotoxic T lymphocyte/target cell interaction: manifestation of a dual activation threshold. *Proc Natl Acad Sci U. S. A.* **100**, 14145–14150 (2003).
53. Delon, J., Bercovici, N., Raposo, G., Liblau, R. & Trautmann, A. Antigen-dependent and -independent Ca2+ responses triggered in T cells by dendritic cells compared with B cells. *J Exp Med.* **188**, 1473–1484 (1998).
54. Kwack, K. B. A new purification method for the Fab and F(ab')2 fragment of 145-2C11, hamster anti-mouse CD3e antibody. *J Biochem Mol Biol.* **33**, 188–192 (2000).

Author contributions

S.N.C. performed the calcium imaging experiments and contributed to the main manuscript text. K.R.D. contributed to and edited the main manuscript text. R.E.N. developed all the computation algorithms and corresponding figures. M.P.B. contributed to the main manuscript text. H.J.G. contributed to the intellectual development of the platforms. K.V. contributed to the intellectual development of the platforms. F.C.C. contributed to the intellectual development of the initial computational algorithms. J.D.H. supervised the project, provided intellectual input and contributed to the main manuscript.

Additional information

Supplementary information accompanies this paper at http://www.nature.com/scientificreports

Competing financial interests: The authors' work resulted in a patent co-operation treaty; International Application No PCT/AU2014/000791, ''ANALYSING INTRACELLULAR CALCIUM FLUX IN CELLS INCLUDING T CELLS'', filed on the 8th of August 2014.

How to cite this article: Christo, S.N. *et al.* Scrutinizing calcium flux oscillations in T lymphocytes to deduce the strength of stimulus. *Sci. Rep.* **5**, 7760; DOI:10.1038/srep07760 (2015).